Mechanical and Viscoelastic Properties of Novel Silk Fibroin Fiber/Poly(ε-Caprolactone) Biocomposites

Wei Li,[1] Xiuying Qiao,[1] Kang Sun,[1] Xiaodong Chen[2]

[1]*State Key Laboratory of Metal Matrix Composites, Shanghai Jiao Tong University, Shanghai 200240, People's Republic of China*
[2]*Shanghai Sunny New Technology Development Company, Limited, Shanghai 201108, China*

Received 19 October 2007; accepted 20 March 2008
DOI 10.1002/app.28514
Published online 16 June 2008 in Wiley InterScience (www.interscience.wiley.com).

ABSTRACT: Silk-fibroin (SF)-fiber-reinforced poly(ε-caprolactone) (PCL) biocomposites with different fiber contents were fabricated by a melt-blending method. The mechanical and viscoelastic properties of these SF/PCL composites were investigated by mechanical property testing, dynamic mechanical thermal analysis, and dynamic rheological analysis. The mechanical properties of PCL were obviously reinforced by fiber addition, and the maximum tensile and flexural strengths appeared at fiber contents of 35 and 45%, respectively. As the fiber content increased, both the storage modulus and loss modulus increased, whereas the glass-transition temperature of the PCL component decreased. The appearance of a storage modulus plateau indicated the formation of reinforcement network structures in the SF/PCL composites, which enhanced the elasticity and viscosity of the composites. The interfacial interaction between the fiber and PCL matrix was not very strong. © 2008 Wiley Periodicals, Inc. J Appl Polym Sci 110: 134–139, 2008

Key words: biomaterials; fibers; rheology

INTRODUCTION

Biodegradable polymer composites consisting of both biodegradable polymers and biodegradable fillers have received more and more attention in recent years because of their potential applications in biomedical and environmental fields. Among these biodegradable polymer matrix composites, the poly(ε-caprolactone) (PCL) based biocomposite is one of the leading examples[1–4] because of its good biocompatibility and good capacity for bone substitutes and drug transport.[5,6]

Natural fibers possess many advantages, such as high strength, low density, high toughness, and good biocompatibility.[7] Therefore, they can be used as biodegradable reinforcements to improve the mechanical properties and control the biodegradability of biocomposites.[8–11] As a kind of natural fiber, silk fiber (*Bombyx mori*) spun out from silkworm cocoons has excellent mechanical properties, such as high tensile strength and modulus, high elongation, good elasticity, and excellent resilience.[12] In a previous study by Lee et al.,[13] raw silk fiber was used to prepare reinforced poly(butylenes succinate) biocomposites, and the effect of fiber content was discussed. *B. mori* silk fiber consists primarily of two protein-based components, the inner fibroin filaments and the outer sericin, which account for about 75 and 25 wt %, respectively.[14] Fibroin, a real fibrous component, is highly crystalline and well aligned in the fiber. Because of the higher mechanical properties of silk fibroin (SF) fiber than those of the sericin, before silk fiber is used, degumming is usually performed to obtain pure fibroin filaments with the removal of the sericin component.[15,16] Biocomposites fabricated with SF fiber are more promising for biomedical fields, especially in bone substitute applications. Moreover, SF also shows outstanding biocompatibility characteristics with living tissues, so SF can be widely used in biotechnological and biomedical applications.[17,18]

Previous studies on SF biocomposites have mainly been related to SF powder rather than the SF fiber.[19–21] In this investigation, the degummed silk fibers as pure fibroin filaments were used to prepare novel SF-fiber-reinforced PCL biocomposites, and the effects of fiber reinforcement on the mechanical and viscoelastic properties of PCL were investigated by static mechanical testing, dynamic mechanical thermal analysis (DMTA), and dynamic rheological analysis.

EXPERIMENTAL

Materials and preparation

PCL, with a number-average molecular weight of 90,000, was purchased from Solvay Group (Brussels, Belgium). Continuous silk fiber was supplied by JinLi

Correspondence to: K. Sun (ksun@sjtu.edu.cn).

TABLE I
Physical Properties of the PCL Matrix and SF Fiber

Material	Density (g/cm^3)	Tensile strength (MPa)	Elongation of at break (%)
PCL	1.16	16.2 ± 0.4	>200
Fiber	1.20	433.0 ± 3.0	12.8 ± 0.2

Silk Co., Ltd. (YuHang, China) and then chopped into short fibers with an approximate length of 1.5 cm in the laboratory. The silk fiber used in this study was spun from the cocoons of *B. mori*.

To remove the sericins, the chopped silk was first degummed by boiling in a 0.5 wt % Na_2CO_3 water solution for 40 min, rinsing in deionized water, and drying *in vacuo* at 70°C for 2 days before use. The physical properties of the PCL matrix and SF fiber are listed in Table I.

SF/PCL composites with different fiber contents were prepared through the melt mixing of PCL and SF fiber at 140°C in a Haake Rheocord900 Rheometer (Haake Mess-Technic GmbH, Karlsruhe, Germany) for 15 min, and then, the obtained composites were hot-pressed in a mold at 140°C and cut into suitable specimens for measurements. Composites with fiber contents of 0, 15, 25, 35, 45, 55, and 65 wt % were denoted as PCL, SP15, SP25, SP35, SP45, SP55, and SP65, correspondingly.

Measurements

An Instron2366 universal tensile tester (Instron Corp., Norwood, Massachusetts, USA) was used for the tensile and flexural tests. The loading rates of both the tensile and flexural measurements were chosen as 1 mm/min. The specimen dimensions for the tensile and flexural measurements were 50 × 4 × 2 and 40 × 15 × 2 mm^3, respectively. The average values of tensile strength, elongation at break, flexural strength, and flexural modulus were determined from five test specimens to evaluate the tensile and flexural properties.

DMTA was performed on a DMTA IV (Rheometric Scientific, Inc., Piscataway, New Jersey, USA) with a three-point bending mode at a fixed frequency of 1 Hz. The testing temperature was controlled from −100 to 30°C at a heating rate of 3°C/min. For each test, the dynamic mechanical property parameters of the storage modulus (E'), the loss modulus (E''), and the loss factor ($\tan \delta = E''/E'$) were obtained as a function of temperature under the conditions of linear viscoelastic response. The number-average molecular weight values of PCL before and after melt mixing were measured by a Series 200 gel permeation chromatograph (PerkinElmer, Inc.).

With the use of a Gemini 200 HR rotational rheometer (Malvern Instruments Inc., Worcestershire, United Kingdom), the dynamic rheological properties were measured on 25-mm parallel plates at 160°C. During the measurements, the strain amplitude was chosen from the linear zone of strain to ensure the linear viscoelastic response, and the dynamic frequency sweep was operated from 100 to 0.01 rad/s to record the viscosity and moduli as a function of angular frequency.

An FEI Sirion 200 scanning electron microscope (FEI Company, Hillsboro, Oregon, USA) was used to examine the microstructures of the SF/PCL composites by observation of the cross sections of the samples fractured in liquid nitrogen. The cross sections were coated with a layer of gold before scanning electron microscopy observation.

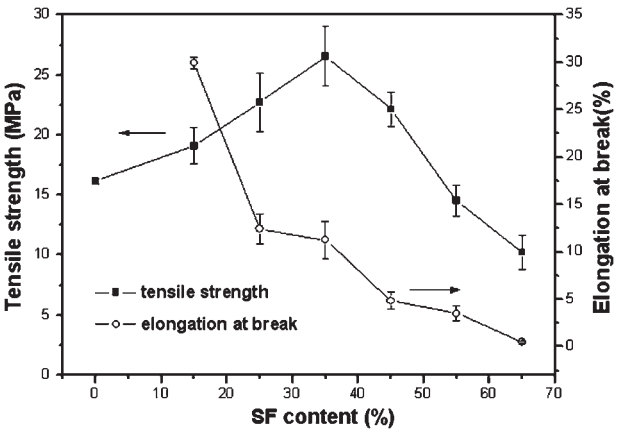

Figure 1 Effect of the SF fiber content on the tensile strength and elongation at break of the SF/PCL composites.

RESULTS AND DISCUSSION

Mechanical properties

Figures 1 and 2 show the mechanical properties of the SF/PCL composites. During the tensile test, PCL

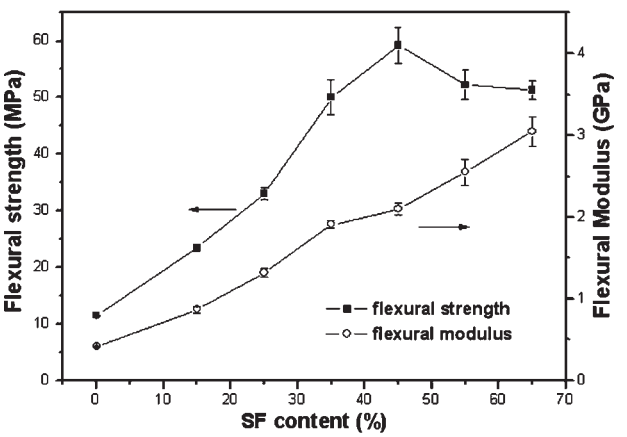

Figure 2 Effect of the SF fiber content on the flexural strength and modulus of the SF/PCL composites.

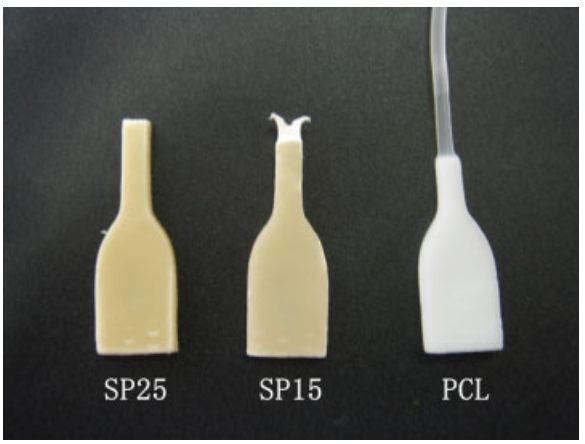

Figure 3 Photographs of PCL, SP15, and SP25 samples after tensile testing. [Color figure can be viewed in the online issue, which is available at www.interscience.wiley.com.]

and SP15 underwent necking and yielding behaviors. However, when the fiber content was higher than 15%, the SF/PCL composites exhibited no necking and yielding behaviors, but they did exhibit brittle fracture behavior, as shown in Figure 3. Just as reflected in Figure 3, the elongation at break of PCL was above 200%, whereas the elongation at break of the SF/PCL composites decreased remarkably with increasing fiber content. Also, the tensile strength of the SF/PCL composites continuously increased with fiber content up to 35% and then decreased with the further addition of fiber.

Similar to the change of tensile strength, with the filling of SF fiber, the flexural strength of the SF/PCL composites also showed a two-stage change, increasing below a fiber content of 45% and then decreasing above a fiber content of 45%. This implied that too much fiber in the composite led to an insufficient coverage of matrix and caused the less effective transfer of external loading from PCL to the fiber and the resultant failure of fiber reinforcement for the PCL matrix. However, the flexural modulus almost linearly increased with the addition of the fiber. The reduction in flexural strength was smaller than that in tensile strength at higher fiber contents. This phenomenon may have been due to the microcracks and defects existing between the fiber–matrix and fiber–fiber phases. Compared with the tensile test, the flexural test was less sensitive to the microcracks and defects.

Dynamic mechanical thermal properties

Figure 4 shows the variation of E', E'', and tan δ as a function of temperature for the PCL matrix and SF/PCL composites. For all samples, the E' curve exhibited a plateau first and then a gradual decrease after the glass transition of the PCL component with increasing temperature. With increasing fiber content, the E' value of the SF/PCL composites increased correspondingly. Moreover, the enhancement of E' over the glass-transition zone of the PCL component was much greater than that below the glass-transition range. In the curves of E'' and tan δ, there was a peak between −60 and −40°C, and the

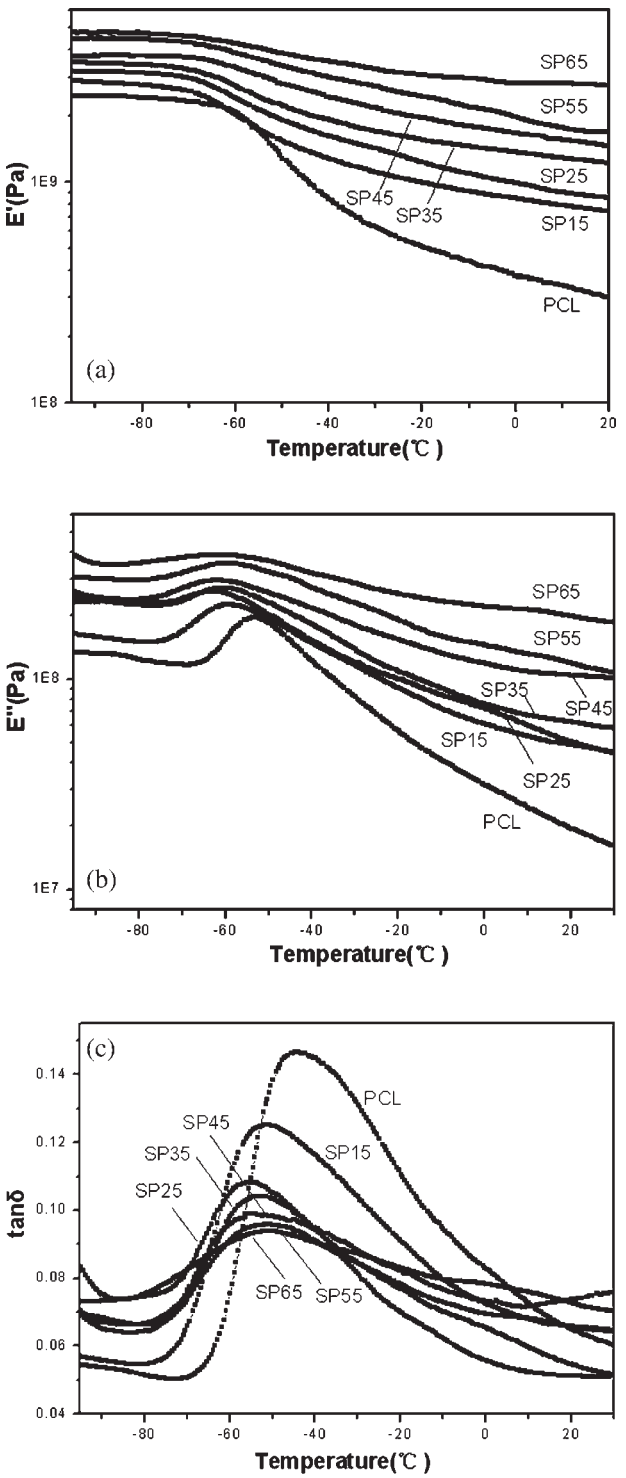

Figure 4 Effect of the SF fiber content on (a) E', (b) E'', and (c) tan δ of the SF/PCL composites.

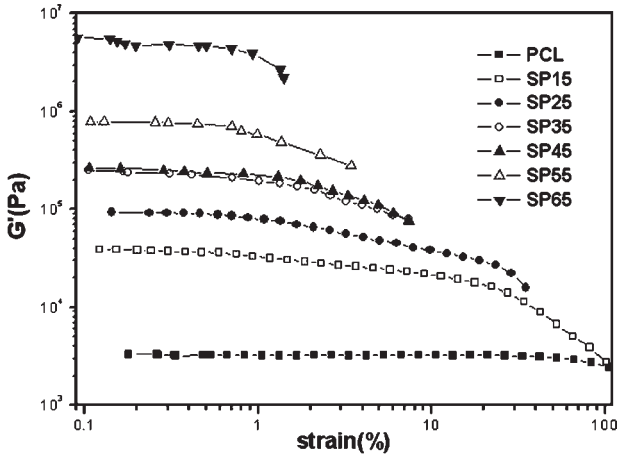

Figure 5 Linear viscoelastic range of the SF/PCL composites.

peak of tan δ could be used to represent the glass-transition temperature of the PCL component. The peak temperature in the tan δ curve was higher than that in the E'' curve, which is a characteristic of semicrystalline polymers. As shown in Figure 4, there was also an obvious glass-transition temperature shift of PCL to lower temperatures with the addition of silk fiber. Through gel permeation chromatography measurements, we found that the number-average molecular weight of PCL changed from 8.923×10^4 to 3.865×10^4 after melt mixing, which indicated the degradation of PCL to some extent during melt-mixing processing. The introduction of fiber filler reduced the interaction of the PCL molecular chains and made the PCL molecular chains move more easily during the phase-transition process, which caused a reduction in the glass-transition temperature.

Linear rheological properties

Rheological analysis is considered an effective tool for the investigation of processing behavior and microstructural features. The responses of the complex viscosity, storage modulus, and loss modulus obtained from rheological analysis provides a better understanding of the processability, dispersion of the filler in the matrix, matrix–fiber interactions, and so on.[22,23]

Before a dynamic frequency sweep, it was necessary to determine the linear viscoelastic range of each sample. Once the linear viscoelastic range is exceeded, the structure of sample is destroyed. Figure 5 shows the storage modulus (G') variation as a function of strain with a frequency of 1 Hz. For all samples, the curves followed the same trend. At low strain, G' showed no effect by strain and then exhibited a drastic drop when a certain strain was reached. In this study, a strain of 0.5% was chosen for the dynamic frequency sweep to measure the linear viscoelastic properties of all of these samples. Figure 5 also shows that as the fiber content increased, G' increased, but the linear range was shortened.

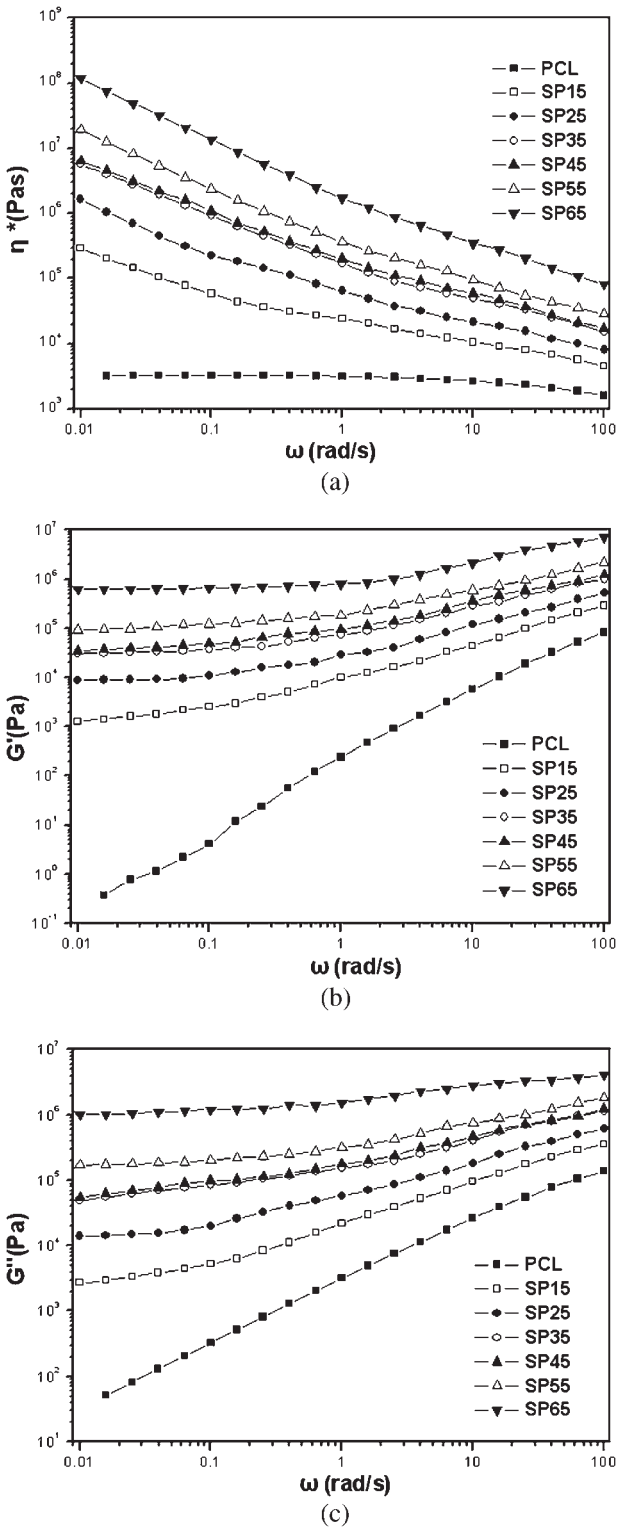

Figure 6 (a) Complex viscosity (η*), (b) G', and (c) G'' of the SF/PCL composites (ω = frequency).

The complex viscosity of the SF/PCL composites as a function of frequency during the dynamic frequency sweep is given in Figure 6. The pure PCL performed as a typical Newtonian fluid in a wide low-frequency range and showed pseudoplastic shear thinning behavior when the frequency increased. After the fibers were blended into the PCL matrix, the low-frequency viscosity plateau of pure PCL disappeared, which implied that the corresponding SF/PCL composited exhibited no Newtonian fluid behavior in the whole testing frequency range. The viscosity increased with increasing fiber content, and the reinforcement effect was more obvious in the low-frequency range than in the high-frequency range. This phenomenon indicated that the fiber played a more dominant role at low oscillatory frequency than at high oscillatory frequency. Meanwhile, when fiber was added to the PCL matrix, the viscosity difference became smaller in the high-frequency range. This phenomenon implied that extrusion and injection were more suitable for the fabrication of the SF/PCL composites.

The G' and loss modulus (G'') values of the SF/PCL composites as a function of frequency are also shown in Figure 6. Like complex viscosity, the modulus also increased with the fiber content, and the reinforcement effect was greater in the low-frequency range than in the high-frequency range. With increasing fiber content, the slope of the modulus became smaller, and a plateau of G' became more obvious. This indicated that when the fiber content increased, a network structure was formed in the SF/PCL composites, which required a higher shear stress and a longer relaxation time for the composite to flow.

When the fiber content was less than 45%, G'' of the SF/PCL composites was higher than G' in the whole test range, which revealed that the viscosity was dominant in these systems. However, when the fiber content reached 45%, a crossover point of G' and G'' appeared. G'' was dominant from the low-frequency range to the crossover point, whereas G' was dominant from the crossover point to the high-frequency range. Figure 7 shows G' and G'' of the SF/PCL composites with fiber contents of 45, 55, and 65%. As shown in Figure 7, the crossover point shifted to a lower frequency with the increase of fiber content, which thus demonstrated that the increase in G' was much greater than the corresponding increase in G'' with increasing fiber concentration. Moreover, the fiber addition changed the rheological behavior of the SF/PCL composites from liquidlike performance to solidlike performance. This phenomenon was mainly ascribed to the network structure formed in the SF/PCL composites, which acted as a reinforced phase and enhanced G' obviously.

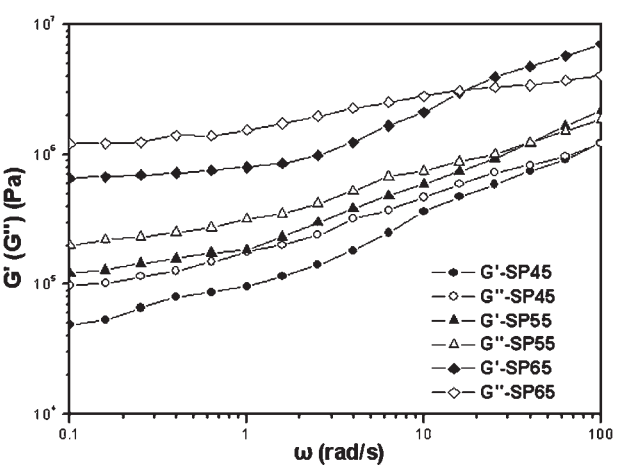

Figure 7 Crossover points of G' and G'' for the SF/PCL composites with fiber contents of 45, 55, and 65 wt % (ω = frequency).

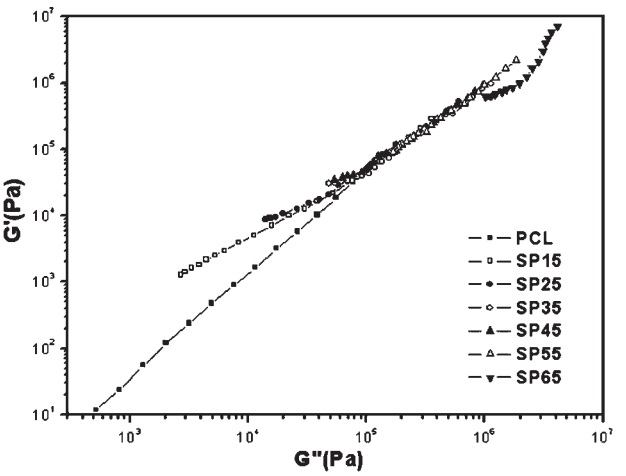

Figure 8 G' as function of G'' for the SF/PCL composites.

A plot of G' versus G'' of melts in an oscillatory flow is an empirical tool for the evaluation of the miscibility of a blend[24] and the interfacial interaction between the reinforced fiber and polymer matrix in a composite.[11] It is suggested that the slope of curves is independent of fiber content if there is a strong interfacial interaction between the fiber and matrix. Figure 8 shows the plots of G' versus G'' for the SF/PCL composites. For the pure PCL, the curve showed a linear relation. After the addition of fiber, the slope of the G'–G'' curves did not change obviously in the high-frequency range but decreased in the low-frequency range, which indicated a weak interfacial interaction between the fiber and the PCL matrix. The weak interfacial interaction may have been due to the different surface natures between the hydrophilic fiber and the hydrophobic PCL matrix.

Morphology observation

Figure 9 shows scanning electron microscopy photographs of the cross sections of liquid-nitrogen-

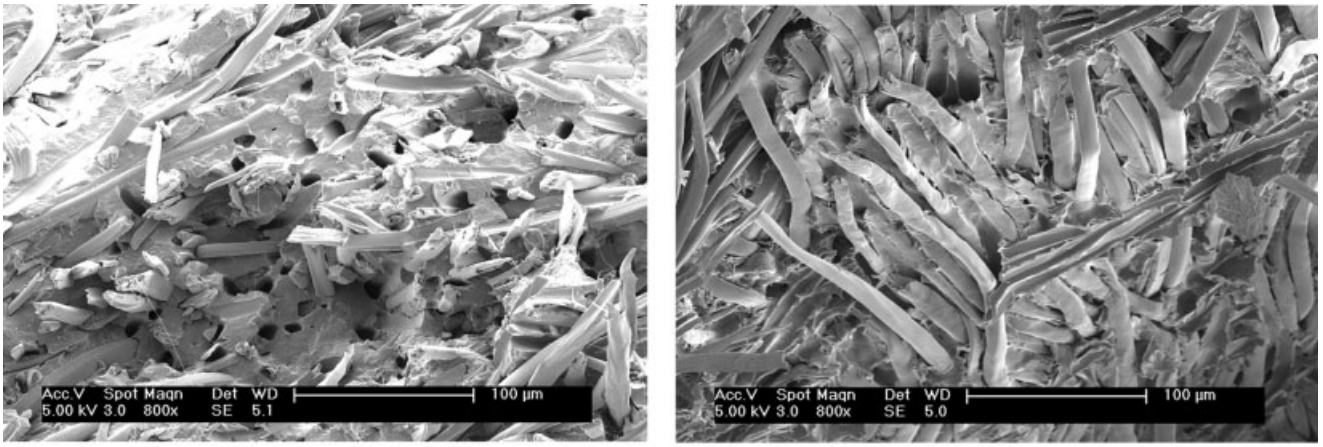

Figure 9 Scanning electron microscopy photographs of cross sections of (a) SP35 and (b) SP55 fractured in liquid nitrogen.

fractured SF/PCL composites with 35 and 55% fiber contents. The diameter of the SF fiber were determined to be about 10 μm. As shown in Figure 9(a), the SF fibers dispersed evenly in the PCL matrix, and the even distribution of fibers may have been beneficial to their reinforcement effect. However, as shown in Figure 9(b), too many fibers led to an insufficient coverage of the matrix and caused the less effective transfer of external loading from PCL to the fiber, which thus resulted in a drop in the tensile and flexural strengths at higher fiber contents during the mechanical test. Moreover, the surfaces of the fiber looked smooth with less PCL matrix on them, which also indicated weak interfacial interactions between the SF fiber and PCL matrix.

CONCLUSIONS

The SF fiber played an important role as a reinforcement phase in improving the mechanical properties of PCL. However, too much fiber caused a drastic drop in the tensile and flexural strengths. As the fiber content increased, both the dynamic modulus and viscosity increased correspondingly. The enhancement effect of the fiber on the storage modulus was higher than that oin the loss modulus. During melt-mixing processing, the degradation of PCL occurred. The viscoelastic data analysis and the morphology observation demonstrated that the interfacial interaction between the fiber and PCL matrix was not very strong.

The authors thank the Instrumental Analysis Center of Shanghai Jiao Tong University for its assistance with the measurements.

References

1. Dell'Erba, R.; Groeninckx, G.; Maglio, G.; Malinconico, M.; Migliozzi, A. Polymer 2001, 42, 7831.
2. Kim, C. H.; Cho, K. Y.; Choi, E. J.; Park, J. K. J Appl Polym Sci 2000, 77, 226.
3. Zhao, J.; Yuan, X.; Cui, Y.; Ge, Q.; Yao, K. J Appl Polym Sci 2004, 91, 1676.
4. Aguilar, C. A.; Lu, Y.; Mao, S.; Chen, S. Biomaterials 2005, 26, 7642.
5. Zhou, S.; Deng, X.; Yang, H. Biomaterials 2003, 24, 3563.
6. Ciapetti, G.; Ambrosio, L.; Savarino, L.; Granchi, D.; Cenni, E.; Baldini, N.; Pagani, S.; Guizzardi, S.; Causa, F.; Giunti, A. Biomaterials 2003, 24, 3815.
7. Mishra, S.; Mohanty, A. K.; Drzal, L. T.; Misra, M.; Parija, S.; Nayak, S. K.; Tripathy, S. S. Compos Sci Technol 2003, 63, 1377.
8. Cyras, V. P.; Kenny, J. M.; Vázquez, A. Polym Eng Sci 2001, 41, 1521.
9. Funabashi, M.; Kunioka, M. Green Chem 2003, 5, 591.
10. Teramoto, N.; Urata, K.; Ozawa, K.; Shibata, M. Polym Degrad Stab 2004, 86, 401.
11. Yang, A.; Wu, R. J Appl Polym Sci 2002, 84, 486.
12. Pérez-Rigueiro, J.; Viney, C.; Llorca, J.; Elices, M. J Appl Polym Sci 1998, 70, 2439.
13. Lee, S. M.; Cho, D.; Park, W. H.; Lee, S. G.; Han, S. O.; Drzal, L. T. Compos Sci Technol 2005, 65, 647.
14. Shao, Z.; Vollrath, F. Nature 2002, 418, 741.
15. Freddi, G.; Mossotti, R.; Innocenti, R. J Biotechnol 2003, 106, 101.
16. Pérez-Rigueiro, J.; Elices, M.; Llorca, J.; Viney, C. J Appl Polym Sci 2002, 84, 1431.
17. Minoura, N.; Aiba, S.; Higuchi, M.; Gotoh, Y.; Tsukada, M.; Imai, Y. Biochem Biophys Res Commun 1995, 208, 511.
18. Demura, M.; Takekawa, T.; Asakura, T.; Nishikawa, A. Biomaterials 1992, 13, 276.
19. Aral, T.; Wilson, D. L.; Kasai, N.; Freddi, G.; Hayasaka, S.; Tsukada, M. J Appl Polym Sci 2002, 84, 1963.
20. Park, S. J.; Lee, K. Y.; Ha, W. S.; Park, S. Y. J Appl Polym Sci 1999, 74, 2571.
21. Chen, G.; Zhou, P.; Mei, N.; Chen, X.; Shao, Z. J Mater Sci: Mater Med 2004, 15, 671.
22. Lozano, K.; Yang, S.; Zeng, Q. J Appl Polym Sci 2004, 93, 155.
23. Pötschke, P.; Fornes, T. D.; Paul, D. R. Polymer 2002, 43, 3247.
24. Han, C. D.; Jhon, M. S. J Appl Polym Sci 1986, 32, 3809.